

Optimized Grid-Connected Hybrid Renewable Energy Power Generation: A Comprehensive Analysis of Photovoltaic, Wind, and Fuel Cell Systems

Mohamed A. J. Al-Ani

CEM Laboratory, National Engineering School of Sfax, University of Sfax, Tunisia
mohalany2@gmail.com

Mohamed Ali Zdiri

CEM Laboratory, National Engineering School of Sfax, University of Sfax, Tunisia
mohamed-ali.zdiri@enis.tn (corresponding author)

Fatma Ben Salem

Prince Sattam Bin Abdulaziz University, College of Engineering, Department of Electrical Engineering, Alkharj, 11942, Saudi Arabia
f.bensalem@psau.edu.sa

Nabil Derbel

CEM Laboratory, National Engineering School of Sfax, University of Sfax, Tunisia
nabil.derbel@enis.tn

Received: 20 January 2024 | Revised: 28 February 2024 and 21 March 2024 | Accepted: 23 March 2024

Licensed under a CC-BY 4.0 license | Copyright (c) by the authors | DOI: <https://doi.org/10.48084/etasr.6936>

ABSTRACT

This paper provides a comprehensive analysis of a grid-connected hybrid microgrid system that seamlessly integrates renewable energy sources, encompassing wind generators, solar arrays, and Fuel Cells (FCs). Emphasis is placed on the pivotal role of power electronic converters in optimizing control and energy management strategies for these diverse sources. The wind and solar subsystems employ Perturb and Observe (P&O) controllers to achieve Maximum Power Point Tracking (MPPT). Additionally, the study delves into the analysis and control design of the grid-connected hybrid system inverter, employing a Proportional-Integral (PI) control technique in the synchronous $d-q$ frame to maximize the output voltage response and active power. In managing renewable grid energy based on artificial neural networks (ANNs), the main goal is to address grid availability concerns by prioritizing renewable sources. The hybrid system acts as a backup during grid unavailability and simultaneously produces hydrogen via electrolysis. The excess energy is seamlessly supplied to the grid upon filling the hydrogen tank. The proposed solution shows great promise for use in renewable energy management systems that combine hybrid technologies.

Keywords-hybrid microgrid system; wind generators; solar arrays; grid; energy management; ANN

I. INTRODUCTION

Hybrid renewable energy systems can incorporate either a single or a combination of RE sources. Various alternative energy sources, including wind, solar, Fuel Cells (FCs), hydropower, biomass, and biogas, improve the efficiency and dependability of the power supply system [1-2]. In addition, FCs can be utilized as secondary energy storage systems with efficiencies superior to those of batteries [3-7]. Most hybrid

renewable energy systems are operated either independently or in conjunction with an existing electricity grid. Standalone systems can cover consumption in geographically isolated areas [8]. However, to combat the unreliability of power grids in areas prone to erratic weather patterns, combination systems are increasingly being recommended and implemented. Numerous studies have proposed and evaluated optimization methods for modeling, optimal sizing, and simulation of hybrid systems, including RE with FCs and grid-connected systems

[9-11]. Many studies on energy management strategies for hybrid grid-connected systems offered valuable insights into the integration of renewable energy sources, control techniques, and optimization approaches. Several studies also highlighted the importance of efficient energy management and seamless integration of renewable sources into hybrid systems [12-17]. Some studies additionally addressed grid availability concerns and proposed backup solutions, such as hydrogen production through electrolysis. However, this approach may have limitations in terms of scope, real-world implementation, data requirements, and potential omissions. Despite these limitations, the specific studies provide a foundation for further research and development in the field of hybrid system energy management, offering promising potential for the efficient utilization of renewable energy in grid-connected systems.

The study comprehensively investigates a grid-connected hybrid microgrid system. It highlights the important role of power electronic converters in optimizing control and energy management strategies by integrating renewable energy sources, such as wind, PVs, and FCs. This study employs P&O controllers in wind and solar systems to implement the MPPT technique and ensure efficient utilization of available renewable energy resources. Furthermore, the current study explores the analysis and control design of a grid-connected hybrid system inverter deploying a Proportional-Integral (PI) control technique in the synchronous $d-q$ frame. This design improves the output voltage response and active power generation, further ameliorating the overall performance of the system. The particular study also introduces an Artificial Neural Network (ANN) controller to address issues on grid availability and prioritize renewable sources. In cases of grid unavailability, the hybrid system serves as a backup while simultaneously producing hydrogen through electrolysis or using previously stored hydrogen to cover the load demand.

The simulation results demonstrate the effectiveness and potential of the proposed approach in hybrid renewable energy management systems, indicating the practical applicability of the proposed method. Comprehensive analysis and integration of various renewable energy sources, along with the utilization of advanced energy management techniques, contribute to the advancement of grid-connected hybrid microgrid systems. The findings of this study have implications for the development and implementation of sustainable and efficient energy systems, promoting the employment of renewable energy and reducing the reliance on conventional power sources.

II. MICROGRID DESCRIPTION

The proposed system, displayed in Figure 1, consists of three distinct sources: PV, wind turbines, and a hydrogen fuel cell. PV production is influenced by both solar irradiation and temperature. To maximize power generation, the MPPT algorithm is employed to track the maximum power achievable from the PV system. The generated power is then connected to a boost converter and subsequently to a DC bus. For the wind energy component, a Permanent Magnet Synchronous Generator (PMSG) is coupled to the wind turbine. Similarly to the PV, the MPPT technique is adopted to optimize power extraction from the wind energy conversion system. The hydrogen FC plays a vital role in the system. Its output is first

fed into a boost converter before being distributed to the DC bus. The DC bus can power DC loads directly, or it can be converted to AC engaging a DC/AC converter. This allows for the distribution of AC power to the grid or other AC devices. By integrating these components, the proposed system enables the efficient utilization of renewable energy sources putting into service switches K1-K6, considering both solar and wind energy. This system configuration demonstrates the potential for effective integration of diverse renewable energy sources, contributing to a more sustainable and reliable energy infrastructure.

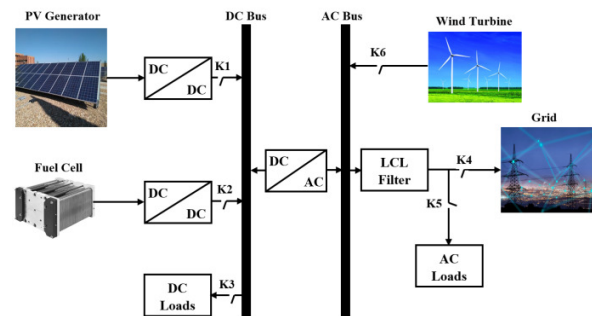


Fig. 1. The studied PV/wind/FC system model connected to the grid.

A. Photovoltaic Array Model

A PV generator is an apparatus that meets load demands by converting solar energy into electricity. When connected in series or parallel, a collection of solar cells forms a PV module. This study employs a one-diode model. The PV generator's equivalent electric circuit is a solar cell. An iterative approach is utilized to perform internal parameter research using datasheet information [18-21]. The output current of the PV array can be mathematically represented as follows [22]:

$$I_{pv} = (I_{sc}N_{pp}) - I_0N_{pp} \exp\left[\frac{qTN_{ss}}{akN_s}\left(V + \frac{IR_s}{N_{pp}}N_{ss}\right) - 1\right] \quad (1)$$

where I_{sc} is the short-circuit cell current, I_0 is the saturation current, q is Boltzmann's constant ($1.381.10^{-23}$ J/K), T is the effective cell temperature, a is the diode quality factor, and q is the electron charge (1.6×10^{-19} C). The numbers of parallel and series PV modules are N_{ss} and N_{pp} , respectively. These goals are met with a DC-DC boost converter managed by MPPT technology. The PV array, which is an AS-6M-350W by Amerisolar-Worldwide Energy and Manufacturing USA Co. Ltd., is suitable for meeting current needs.

B. DC-DC Boost Converter

The fundamental circuit components of the DC-DC boost topology were discussed in [23]. When calculating the inductance and capacitors (L , C_e , and C_s), it is important to take into account that the output voltage is 600 V.

C. MPPT Controller

The MPPT DC-DC converter is frequently used to optimize the PV array power [24]. By measuring the PV system's current I_{pv} , voltage V_{pv} , and power P_{pv} , the Perturbation and

Observation (P&O) technique's maximum power point can be followed and act as a reference in the following study.

D. DC-AC Converter

Figure 2 displays a representation of the DC/AC converter circuit, which utilizes either Insulated Gate Bipolar Transistors (IGBTs) or diode bridges as the primary components [25-27].

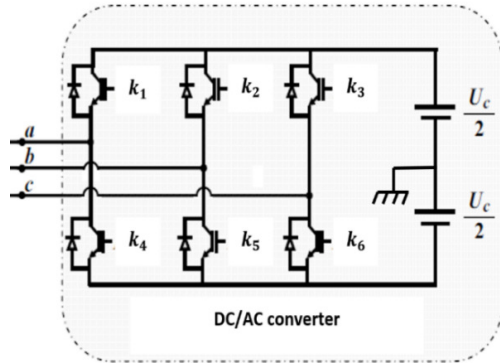


Fig. 2. DC/AC converter circuit.

E. PMSM Model

The dynamic behavior of a PMSM is defined in terms of space variables in the following manner [28]:

$$\bar{V}_{abc} = R_s \bar{I}_{abc} + L_s \frac{d}{dt} \bar{I}_{abc} + \frac{d}{dt} \Phi_{mabc} \quad (2)$$

The PMSM's mechanical equation can be described as follows:

$$J \frac{d}{dt} \Omega_m = T_{em} - T_l \quad (3)$$

where J represents the inertia of the motor, T_{em} represents the electromagnetic torque, and T_l represents the load torque.

F. Features of Wind Turbines

Figure 3 indicates that the wind speed has the greatest impact on the wind turbine's power output. Wind power is a cubic function of wind speed. Thus, changes in wind speed have a significant impact on power.

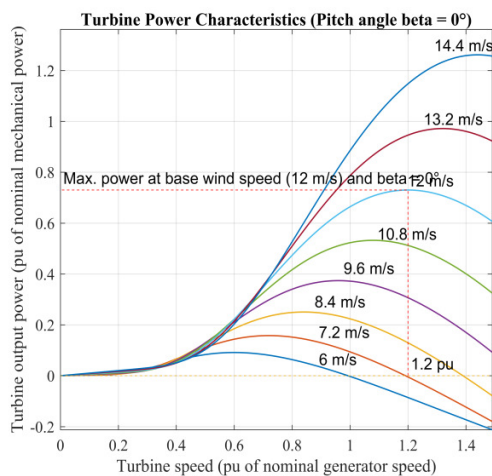


Fig. 3. Wind turbine power characteristics.

III. ELECTRICAL GRID

A. The LCL Filter

Grid-tied inverters have high switching harmonics and no filter. The voltage of the electrical grid drops when such currents are transmitted to it without a filter, causing many power quality problems. A high-quality LCL filter can be applied to the inverter output to prevent power quality issues. Thus, the inverter output side can generate harmonic-free electricity with a smooth sinusoidal current. Figure 4 demonstrates that grid-tied inverters prefer LCL filters due to their low cost and high performance. The inverter ripple current is limited by $L1$, the current-carrying inductor on the inverter side. The common range for the ripple current is 10-15% of the rated current.

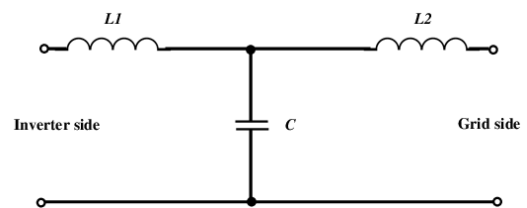


Fig. 4. LCL filter block.

B. DQ Control Strategy

Figure 5 depicts a schematic of the DQ control used. DQ control, also known as Park's transformation, is a commonly employed control method in electrical systems to facilitate the control of three-phase AC quantities in a two-phase reference frame [29].

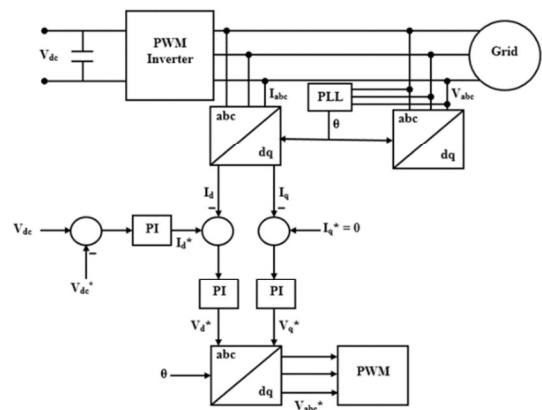


Fig. 5. General structure of DQ control.

C. PLL

Figure 6 portrays the three-phase PLL block diagram. The observed grid voltage (V_{abc}) is transformed to DC components using the abc/dq coordinate transformation. To lock the PLL, V_d^* is considered to be zero. A low-pass filter appears to be the PI loop filter. The integrator Voltage-Controlled Oscillator (VCO) receives a DC-regulated signal with a suppressed high-frequency component. The inverter phase angle is calculated by integrating the output frequency of the PI controller. When the

PLL is operational, the difference between the grid and inverter phase angles is reduced to zero. The voltages rotate simultaneously, with $V_d = 0$ and V_q indicating the magnitude of the grid voltage.

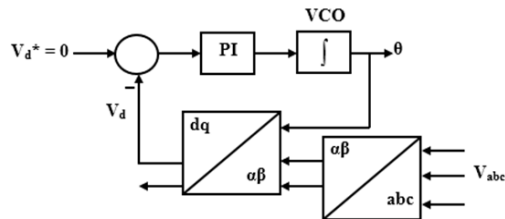


Fig. 6. PLL general structure.

IV. ENERGY MANAGEMENT APPROACH

The challenge of energy management is delineated through the mathematical representation of a comprehensive control approach that involves inputs, outputs, objectives, and constraints. This study aims to implement renewable energy sources as a solution to address grid availability concerns. Consequently, three scenarios emerge based on the grid status:

- Scenario I: When the grid is accessible, it serves as the sole power source to meet the load demand. The power generated by the PV system and wind turbines is harnessed by the electrolyzer to produce hydrogen. The excess energy is then sold as an additional benefit to the grid once the tanks are full.
- Scenario II: In cases where the grid is unavailable and there is an excess of renewable electricity over the load requirement, the excess power is sent to the electrolyzer to be converted into hydrogen. The extra power is discharged through a dump load if the hydrogen tanks are full.
- Scenario III: When the load demand exceeds the power generated by the PV system and the wind turbine, and the grid is unavailable, the power is obtained from previously stored hydrogen through fuel cells. Any power deficit will be assessed if fuel cells are unable to meet the required load.

This study focuses on the system design for making connection decisions between the hybrid system and the grid to meet their respective loads. Several criteria were considered to ensure an effective management algorithm, as shown in Figure 7. It is important to note that the grid is consistently available in this particular scenario and the total renewable energy system, consisting of both PV and wind systems, is denoted as P_{pw} in this context. Recently, there has been a growing interest in employing machine learning for hybrid systems connected to grids. This technique relies on ANNs to address complex problems [30]. The ANN model has two critical stages: training and operation. The ANN model inputs are renewable energy sources, FC, and the grid, along with their switching statuses (on or off). ANN model development occurs in MATLAB/SIMULINK. The feedforward neural network has three input neurons, seven hidden neurons, and three output neurons, as detected in Figure 8.

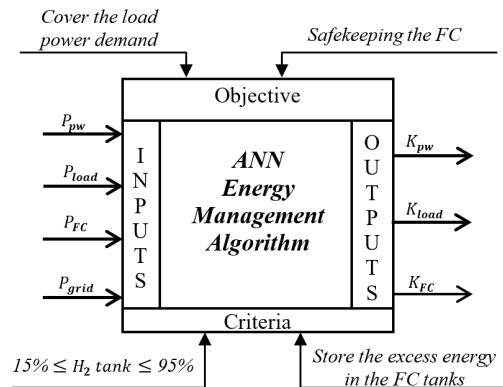


Fig. 7. The ANN synoptic schema.

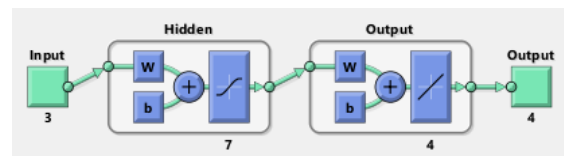


Fig. 8. Feedforward NN model using MATLAB/SIMULINK.

Simulated data points from the grid-connected hybrid renewable energy system were deployed for training purposes, employing the Levenberg-Marquardt algorithm. The training performance curve demonstrates the progress of the training process, with the Mean Squared Error (MSE) reaching an impressive value of 9.7302×10^{-10} at epoch 257, as exhibited in Figure 9. These achievements contribute to the high performance of flux transfer and ensure the uninterrupted supply of power to both AC and DC loads.

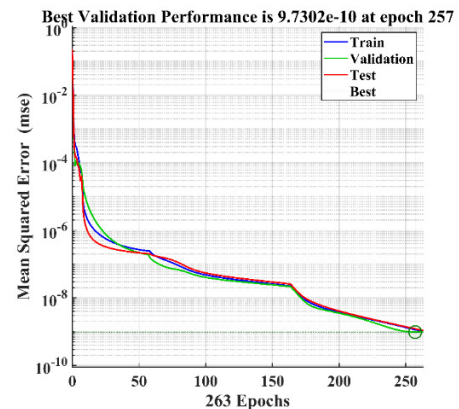


Fig. 9. Feedforward NN performance.

V. SIMULATION ANALYSIS AND RESULTS

A. Application

This study puts into service a 1.5 MW wind turbine and a 1.5 MW PV generator. Table I demonstrates the parameters for the grid-connected hybrid system.

TABLE I. SYSTEM PARAMETERS

PV generator parameters	
Maximum power	1.5 MW
Voltage at MPP	300
Current at MPP	5000
Wind parameters	
Rated Power	1.5 MW
Air density	1.225 kg/m ³
Rated wind speed	12 m/sec
FC Parameters	
Fuel type	Hydrogen
Efficiency	>50%
Grid parameters	
Voltage and frequency	400 V, 50 Hz

B. Simulation Results

The proposed system was simulated utilizing MATLAB/SIMULINK, as illustrated in Figure 10. Figure 11 depicts the climate condition profiles for both PV and wind energy sources. These profiles provide an overview of the weather patterns and characteristics that affect the generation of electricity from solar and wind resources.

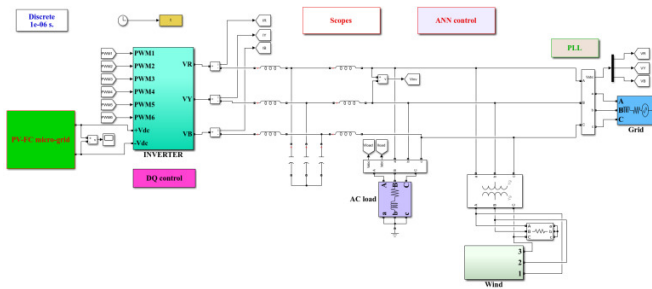


Fig. 10. MATLAB/SIMULINK simulation model of the proposed system.

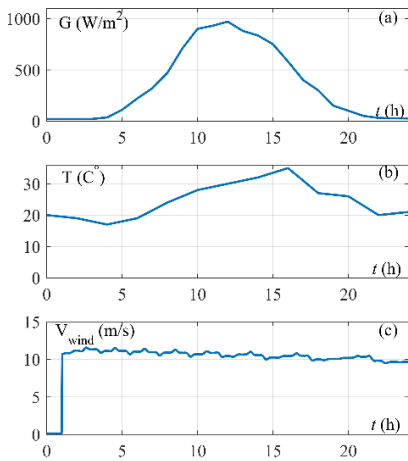


Fig. 11. Climatic conditions profile.

Figure 12 reveals the variations in PV and wind powers (P_{gp} and P_{wind}). It is important to note that the power of renewable sources closely follows the trajectory of the climate conditions, which can be attributed to the utilization of the P&O technique. The P&O MPPT technique enables the system to efficiently track and extract the maximum available power from PV and

wind sources, aligning their power generation with the prevailing climatic conditions. Figure 13 represents the total source power and the DC voltage.

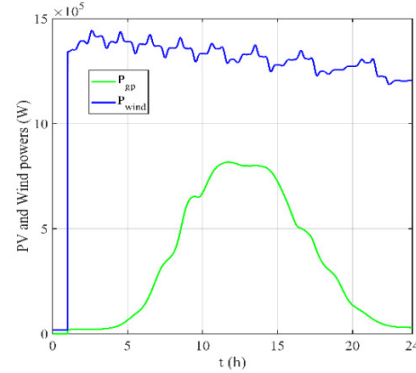


Fig. 12. PV and wind power.

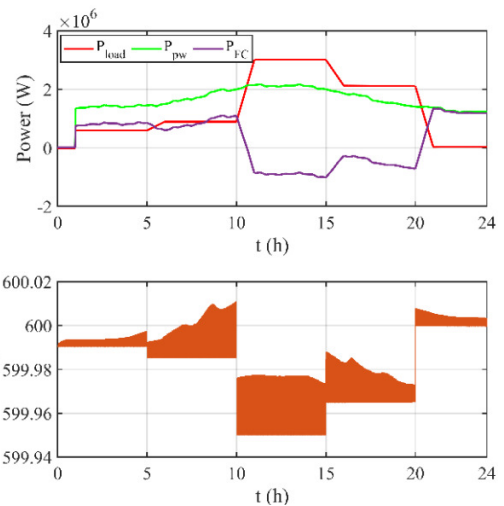


Fig. 13. The source power and DC voltage during 24 hours.

Figure 13 clearly shows that the power consumed by the load (P_{load}) is derived from the combined power of renewable energy sources (P_{pw}) and the power generated by the fuel cell (P_{FC}). As a result, the voltage remains constant despite fluctuations in climatic conditions. This observation highlights the effectiveness and high performance of the proposed management system. The ability to maintain constant voltage despite varying weather conditions demonstrates the successful integration and coordination of renewable energy sources and FCs within the system. In addition to improving the system's overall efficiency and dependability, this steady voltage output guarantees a steady power supply to the load. The stability of the system and the uninterrupted power supply to the load are demonstrated by the capacity of the proposed management system to optimize the use of renewable energy sources and the FC while efficiently controlling the power flow.

Considering the proposed management strategy and the variations in climatic conditions and load, the fluctuation in the continuous bus voltage is estimated to be around 1% of the reference voltage of 600 V. This indicates that the system

maintains a relatively stable bus voltage, with minor deviations within an acceptable range considering the given conditions compared to other existing studies.

Figure 14 portrays the operation of the switches in the proposed system according to the suggested ANN management strategy. It is important to emphasize that K_{pw} is equal to K1 and K6, K_{FC} is equal to K2, and K_{load} is equal to K3 and K4. Additionally, it should be noted that the K_{FC} switcher is an Insulated Gate Bipolar Transistor (IGBT) antiparallel with a diode. On examining the figure, it becomes evident that when there is an excess of renewable energy, the FC charges. Conversely, when there is insufficient energy from renewable sources, the FC discharges can meet the energy requirements of both AC and DC loads.

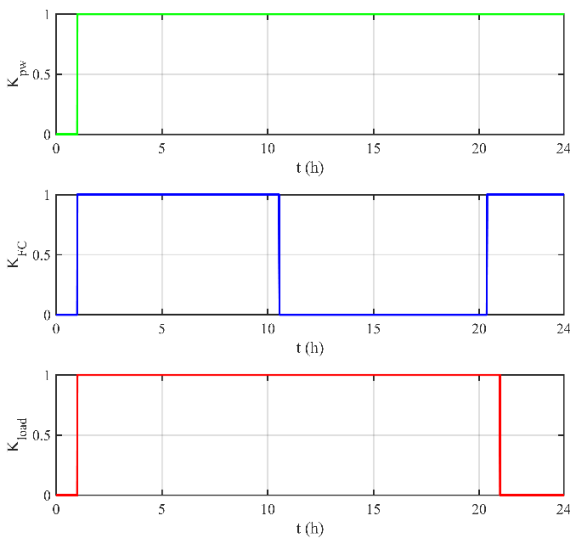


Fig. 14. Switches operation.

Figure 15 provides a comprehensive analysis of the inverter's performance, highlighting its successful delivery of an active power of 1.45×10^5 W to the electrical grid. The closed-loop current control mechanism ensures the absence of reactive power, maintaining a unity power factor during power transfer from the PV, wind, and FC sources. Remarkably, when faced with an inductive load, the inverter efficiently responds to the reactive power requirements, resulting in negative reactive power rather than zero. This highlights the inverter's ability to effectively manage reactive power flow and optimize power delivery to the grid. The inverter's capability to handle both active and reactive power ensures a reliable and efficient power supply to meet the grid's demands. Figure 16 presents the waveforms of the phase-phase voltage and single-phase current of the RL load. These waveforms provide essential information regarding the load's behavior and performance, facilitating the analysis of its power consumption and electrical characteristics. The phase-phase voltage waveform offers insights into the voltage levels and fluctuations experienced across the load. By observing this waveform, variations in voltage magnitude, frequency, and any potential distortions can be identified, enabling a better understanding of the load's voltage requirements and the quality of the supplied power.

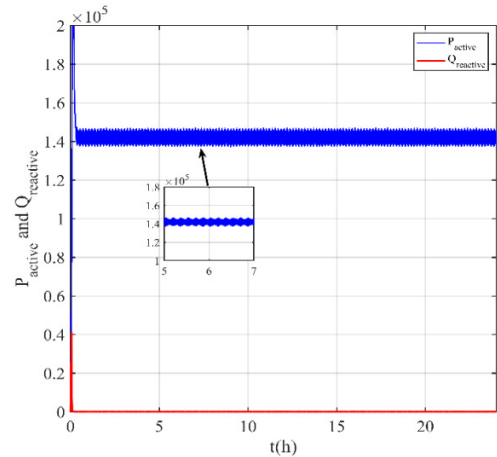


Fig. 15. Active and reactive power.

Furthermore, the single-phase current waveform provides valuable insights into the load's behavior and performance over time. This waveform enables the analysis of crucial parameters, such as the power factor, harmonic content, and any irregularities that could indicate potential issues or inefficiencies in the load's operation. By examining the current waveform, it becomes possible to identify and address any power quality concerns, optimize load performance, and ensure efficient utilization of electrical energy. The waveform serves as a valuable tool for monitoring and troubleshooting load operations, facilitating the identification of areas for improvement in terms of power factor correction, harmonic mitigation, and overall load efficiency.

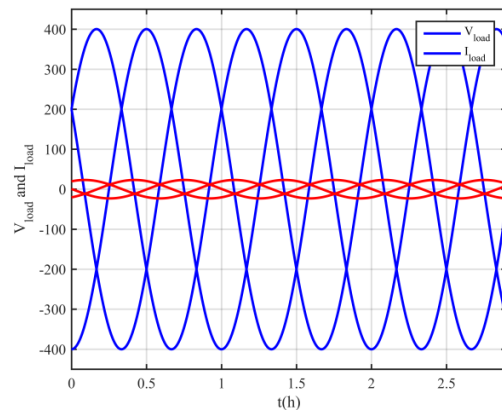


Fig. 16. Load voltage and current.

Figure 17 displays the Fast Fourier transform (FFT) analysis of the inverter's output current, revealing an impressively low Total Harmonic Distortion (THD) level of 1.73% according to the proposed strategy. This signifies the inverter's exceptional performance in converting DC power to AC output with minimal distortion and negligible higher-order harmonic interference. The results validate the efficacy of the inverter control design and demonstrate its superiority compared to existing studies in the field [31-32]. The low THD value highlights the inverter's ability to generate a clean and

high-quality AC output, ensuring the delivery of reliable power to connected loads while minimizing the risk of electrical disturbances and potential equipment malfunctions.

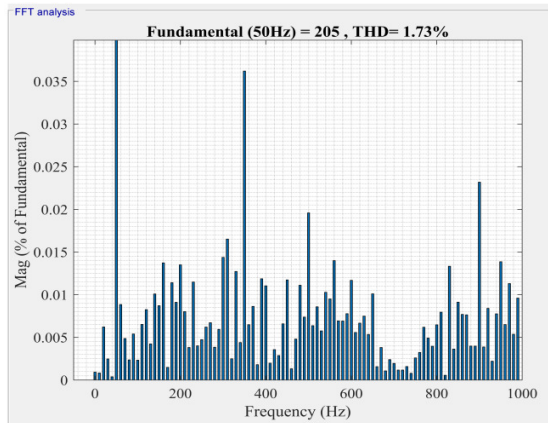


Fig. 17. Total harmonic distortions (THD).

VI. CONCLUSION

This study aimed to provide a comprehensive analysis of a grid-connected hybrid renewable energy system that integrates wind, solar, and hydrogen fuel cell technologies. The current study focused on the crucial role of power electronic converters in optimizing control and energy management strategies. A backup system that involves hydrogen production and a seamless supply of excess energy to the grid was proposed. This approach was designed to improve grid reliability and effectively manage renewable energy sources by ensuring continuous power supply during periods of low renewable energy availability. The novel management strategy proposed for the grid-connected hybrid renewable energy system used an ANN controller. The results obtained from this strategy highlight its effectiveness, as indicated by a low THD value of 1.73% and consistent voltage regulation even during varying climatic conditions of wind and solar sources. This remarkable achievement highlights the exceptional performance and efficiency of the proposed system when implementing the recommended management approach. Although this study has made significant strides in the field, several future research directions are identified, including:

- Advanced control techniques
- Grid interaction and stability
- Economic analysis.

It is important to address these future research points to create a more sustainable and resilient energy future. This will help advance and practically deploy grid-connected hybrid renewable energy systems.

ACKNOWLEDGEMENT

This paper is supported via funding from Prince Sattam Bin Abdulaziz University, Project Number (PSAU/2024/R/1445).

REFERENCES

- [1] T. Z. Ang, M. Salem, M. Kamarol, H. S. Das, M. A. Nazari, and N. Prabakaran, "A comprehensive study of renewable energy sources: Classifications, challenges and suggestions," *Energy Strategy Reviews*, vol. 43, Sep. 2022, Art. no. 100939, <https://doi.org/10.1016/j.esr.2022.100939>.
- [2] H. Stančin, H. Mikulčić, X. Wang, and N. Duić, "A review on alternative fuels in future energy system," *Renewable and Sustainable Energy Reviews*, vol. 128, Aug. 2020, Art. no. 109927, <https://doi.org/10.1016/j.rser.2020.109927>.
- [3] B. Bendjedja, N. Rizoug, M. Boukhniifer, F. Bouchafaa, and M. Benbouzid, "Influence of secondary source technologies and energy management strategies on Energy Storage System sizing for fuel cell electric vehicles," *International Journal of Hydrogen Energy*, vol. 43, no. 25, pp. 11614–11628, Jun. 2018, <https://doi.org/10.1016/j.ijhydene.2017.03.166>.
- [4] Z. Zhang *et al.*, "A review of technologies and applications on versatile energy storage systems," *Renewable and Sustainable Energy Reviews*, vol. 148, Sep. 2021, Art. no. 111263, <https://doi.org/10.1016/j.rser.2021.111263>.
- [5] M. Tawalbeh, S. Z. M. Murtaza, A. Al-Othman, A. H. Alami, K. Singh, and A. G. Olabi, "Ammonia: A versatile candidate for the use in energy storage systems," *Renewable Energy*, vol. 194, pp. 955–977, Jul. 2022, <https://doi.org/10.1016/j.renene.2022.06.015>.
- [6] M. U. Mutarraf, Y. Terriche, K. A. K. Niazi, J. C. Vasquez, and J. M. Guerrero, "Energy Storage Systems for Shipboard Microgrids—A Review," *Energies*, vol. 11, no. 12, Dec. 2018, Art. no. 3492, <https://doi.org/10.3390/en11123492>.
- [7] M. Yekini Suberu, M. Wazir Mustafa, and N. Bashir, "Energy storage systems for renewable energy power sector integration and mitigation of intermittency," *Renewable and Sustainable Energy Reviews*, vol. 35, pp. 499–514, Jul. 2014, <https://doi.org/10.1016/j.rser.2014.04.009>.
- [8] E. I. Come Zebra, H. J. van der Windt, G. Nhumaio, and A. P. C. Faaij, "A review of hybrid renewable energy systems in mini-grids for off-grid electrification in developing countries," *Renewable and Sustainable Energy Reviews*, vol. 144, Jul. 2021, Art. no. 111036, <https://doi.org/10.1016/j.rser.2021.111036>.
- [9] M. Thirunavukkarasu, Y. Sawle, and H. Lala, "A comprehensive review on optimization of hybrid renewable energy systems using various optimization techniques," *Renewable and Sustainable Energy Reviews*, vol. 176, Apr. 2023, Art. no. 113192, <https://doi.org/10.1016/j.rser.2023.113192>.
- [10] S. M. Dawoud, X. Lin, and M. I. Okba, "Hybrid renewable microgrid optimization techniques: A review," *Renewable and Sustainable Energy Reviews*, vol. 82, pp. 2039–2052, Feb. 2018, <https://doi.org/10.1016/j.rser.2017.08.007>.
- [11] M. S. Okundamiya, "Size optimization of a hybrid photovoltaic/fuel cell grid connected power system including hydrogen storage," *International Journal of Hydrogen Energy*, vol. 46, no. 59, pp. 30539–30546, Aug. 2021, <https://doi.org/10.1016/j.ijhydene.2020.11.185>.
- [12] A. Elmoutamid, R. Ouladsine, M. Bakhouya, N. El Kamoun, M. Khaidar, and K. Zine-Dine, "Review of Control and Energy Management Approaches in Micro-Grid Systems," *Energies*, vol. 14, no. 1, Jan. 2021, Art. no. 168, <https://doi.org/10.3390/en14010168>.
- [13] D.-D. Tran, M. Vafaipour, M. El Baghdadi, R. Barrero, J. Van Mierlo, and O. Hegazy, "Thorough state-of-the-art analysis of electric and hybrid vehicle powertrains: Topologies and integrated energy management strategies," *Renewable and Sustainable Energy Reviews*, vol. 119, Mar. 2020, Art. no. 109596, <https://doi.org/10.1016/j.rser.2019.109596>.
- [14] A. Merabet, A. Al-Durra, and E. F. El-Saadany, "Energy management system for optimal cost and storage utilization of renewable hybrid energy microgrid," *Energy Conversion and Management*, vol. 252, Jan. 2022, Art. no. 115116, <https://doi.org/10.1016/j.enconman.2021.115116>.
- [15] K. Njeh, M. A. Zdiri, M. B. Ammar, A. Rabhi, and F. B. Salem, "Energy Management of an Autonomous Photovoltaic System under Climatic Variations," *Engineering, Technology & Applied Science Research*, vol.

- 13, no. 1, pp. 9849–9854, Feb. 2023, <https://doi.org/10.48084/etasr.5375>.
- [16] T. V. Krishna, M. K. Maharana, and C. K. Panigrahi, "Integrated Design and Control of Renewable Energy Sources for Energy Management," *Engineering, Technology & Applied Science Research*, vol. 10, no. 3, pp. 5857–5863, Jun. 2020, <https://doi.org/10.48084/etasr.3613>.
- [17] S. Sarwar, D. Kirli, M. M. C. Merlin, and A. E. Kiprakis, "Major Challenges towards Energy Management and Power Sharing in a Hybrid AC/DC Microgrid: A Review," *Energies*, vol. 15, no. 23, Jan. 2022, Art. no. 8851, <https://doi.org/10.3390/en15238851>.
- [18] M. A. Zdiri, B. Dhouib, Z. Alaas, F. B. Salem, and H. H. Abdallah, "Load Flow Analysis and the Impact of a Solar PV Generator in a Radial Distribution Network," *Engineering, Technology & Applied Science Research*, vol. 13, no. 1, pp. 10078–10085, Feb. 2023, <https://doi.org/10.48084/etasr.5496>.
- [19] R. K. Pachauri *et al.*, "Impact of Partial Shading on Various PV Array Configurations and Different Modeling Approaches: A Comprehensive Review," *IEEE Access*, vol. 8, pp. 181375–181403, 2020, <https://doi.org/10.1109/ACCESS.2020.3028473>.
- [20] M. F. Jalil, S. Khatoun, I. Nasiruddin, and R. C. Bansal, "Review of PV array modelling, configuration and MPPT techniques," *International Journal of Modelling and Simulation*, vol. 42, no. 4, pp. 533–550, Jul. 2022, <https://doi.org/10.1080/02286203.2021.1938810>.
- [21] S. Kichou, S. Silvestre, L. Guglielminotti, L. Mora-López, and E. Muñoz-Cerón, "Comparison of two PV array models for the simulation of PV systems using five different algorithms for the parameters identification," *Renewable Energy*, vol. 99, pp. 270–279, Dec. 2016, <https://doi.org/10.1016/j.renene.2016.07.002>.
- [22] M. Kermadi, V. J. Chin, S. Mekhilef, and Z. Salam, "A fast and accurate generalized analytical approach for PV arrays modeling under partial shading conditions," *Solar Energy*, vol. 208, pp. 753–765, Sep. 2020, <https://doi.org/10.1016/j.solener.2020.07.077>.
- [23] A. Al-Ateeq and A. J. Alateeq, "Soft-Charging Effects on a High Gain DC-to-DC Step-up Converter with PSC Voltage Multipliers," *Engineering, Technology & Applied Science Research*, vol. 10, no. 5, pp. 6323–6329, Oct. 2020, <https://doi.org/10.48084/etasr.3773>.
- [24] M. L. Katche, A. B. Makokha, S. O. Zachary, and M. S. Adaramola, "A Comprehensive Review of Maximum Power Point Tracking (MPPT) Techniques Used in Solar PV Systems," *Energies*, vol. 16, no. 5, Jan. 2023, Art. no. 2206, <https://doi.org/10.3390/en16052206>.
- [25] H. Sathishkumar and S. S. Parthasarathy, "Space vector pulse width modulation for DC-AC converter," in *2016 Second International Conference on Science Technology Engineering and Management (ICONSTEM)*, Chennai, India, Mar. 2016, pp. 310–314, <https://doi.org/10.1109/ICONSTEM.2016.7560968>.
- [26] P. B. Shinde and T. N. Date, "Pulse width modulation control of 3 phase AC-AC matrix converter," in *2017 International Conference on Computing Methodologies and Communication (ICCMC)*, Erode, India, Jul. 2017, pp. 992–997, <https://doi.org/10.1109/ICCMC.2017.8282618>.
- [27] X. Li, X. Ruan, Q. Jin, M. Sha, and C. K. Tse, "Approximate Discrete-Time Modeling of DC-DC Converters With Consideration of the Effects of Pulse Width Modulation," *IEEE Transactions on Power Electronics*, vol. 33, no. 8, pp. 7071–7082, Dec. 2018, <https://doi.org/10.1109/TPEL.2017.2752419>.
- [28] B. Dhouib, M. A. Zdiri, Z. Alaas, and H. H. Abdallah, "Analyzing the Effects of MBPSS on the Transit Stability and High-Level Integration of Wind Farms during Fault Conditions," *Engineering, Technology & Applied Science Research*, vol. 13, no. 3, pp. 10652–10658, Jun. 2023, <https://doi.org/10.48084/etasr.5838>.
- [29] L. Peng, L. Ma, W. Song, and H. Liu, "Reference-input-based imaginary axis current estimation method for DQ control strategy of single-phase PWM converters," *CSEE Journal of Power and Energy Systems*, pp. 1–9, 2022, <https://doi.org/10.17775/CSEEJPES.2020.04220>.
- [30] S. Xie, X. Hu, S. Qi, and K. Lang, "An artificial neural network-enhanced energy management strategy for plug-in hybrid electric vehicles," *Energy*, vol. 163, pp. 837–848, Nov. 2018, <https://doi.org/10.1016/j.energy.2018.08.139>.
- [31] B. Dhouib, M. A. Zdiri, Z. Alaas, and H. Hadj Abdallah, "Fault Analysis of a Small PV/Wind Farm Hybrid System Connected to the Grid," *Applied Sciences*, vol. 13, no. 3, Jan. 2023, Art. no. 1743, <https://doi.org/10.3390/app13031743>.
- [32] H. Zang *et al.*, "Hybrid method for short-term photovoltaic power forecasting based on deep convolutional neural network," *IET Generation, Transmission & Distribution*, vol. 12, no. 20, pp. 4557–4567, 2018, <https://doi.org/10.1049/iet-gtd.2018.5847>.